frontiers | Frontiers in Nanotechnology

TYPE Original Research
PUBLISHED 11 October 2022
DOI 10.3389/fnano.2022.988997

OPEN ACCESS

EDITED BY
Virginie Ponsinet,
UPR8641 Centre de Recherche Paul Pascal (CRPP), France

REVIEWED BY
Carole Ecoffet,
UMR7361 Institut de Sciences des Matériaux de Mulhouse, France
Shih-Hsin Hsu,
Purdue University, United States

*CORRESPONDENCE
John T. Fourkas,
fourkas@umd.edu

†These authors have contributed equally to this work

SPECIALTY SECTION
This article was submitted to Nanofabrication, a section of the journal Frontiers in Nanotechnology

RECEIVED 07 July 2022
ACCEPTED 16 September 2022
PUBLISHED 11 October 2022

CITATION
Liaros N, Tomova Z, Gutierrez Razo SA, Bender JS, Souna AJ, Devoe RJ, Ender DA, Gates BJ and Fourkas JT (2022), Thermal feature-size enhancement in multiphoton photoresists. *Front. Nanotechnol.* 4:988997. doi: 10.3389/fnano.2022.988997

Thermal feature-size enhancement in multiphoton photoresists

Nikolaos Liaros[1†], Zuleykhan Tomova[1†], Sandra A. Gutierrez Razo[1†], John S. Bender[1], Amanda J. Souna[1], Robert J. Devoe[2], David A. Ender[2], Brian J. Gates[2] and John T. Fourkas[1,3,4,5*]

[1]Department of Chemistry and Biochemistry, University of Maryland, College Park, MD, United States, [2]Corporate Research Process Laboratory, 3M Co, 208-1-1 3M Center, St. Paul, MN, United States, [3]Institute for Physical Science and Technology, University of Maryland, College Park, MD, United States, [4]Maryland Quantum Materials Center, University of Maryland, College Park, MD, United States, [5]Maryland NanoCenter, University of Maryland, College Park, MD, United States

We demonstrate a new approach for decreasing the feature size in multiphoton absorption polymerization (MAP). Acrylic photoresists containing the photoinitiator KL68 (bis-[4-(diphenylamino) stryl]-1-(2-ethylhexyloxy), 4-(methoxy)benzene) exhibit a proportional velocity (PROVE) dependence, yielding smaller feature sizes at lower fabrication speeds. The feature size in this photoresist decreases substantially with a temperature increase of less than 10°C when all other fabrication parameters are kept constant, suggesting that the PROVE behavior results from local heating. Although higher temperatures have previously been associated with decreased feature sizes in MAP, the effect observed here is considerably stronger than in previous work, and is shown to be a property of the photoinitiator. This discovery opens the door to exploiting thermal gradients to improve resolution in MAP lithography.

KEYWORDS

multiphoton absorption polymerization, photopolymerization, resolution enhancement, thermal effects, proportional velocity dependence

Introduction

There is currently a tremendous demand for the rapid prototyping and manufacture of three-dimensional (3D) parts with feature sizes as small as a few tens of nanometers (Fourkas et al., 2021), for use in application spaces such as microelectronics (Camposeo et al., 2019), photonics (Campbell et al., 2000), biomedicine (Pan and Wang, 2011), the automotive industry (Finkbeiner, 2013), and telecommunications (Wu et al., 2015). The ability to fabricate geometrically complex structures using a broad range of materials has made additive manufacturing techniques attractive means for microfabrication (Ngo et al., 2018). Multiphoton absorption polymerization (MAP) is a unique approach to additive manufacturing, given this technique's high resolution and its inherent 3D fabrication capability for structures with complex geometries (Lafratta et al., 2007).

MAP is most often performed using negative-tone photoresists, which are materials that become cross-linked, and therefore insoluble, upon sufficient exposure to light. Typical acrylic photoresists consist of a mixture of multifunctional monomers and a radical photoinitiator. Upon photoexcitation, the photoinitiators generate radicals, leading to a cross-linking chain reaction that, with sufficient exposure, renders the material insoluble.

Due to the nonlinear nature of multiphoton excitation, the polymerization reaction is contained within the focal volume of a tightly focused laser beam, where the crosslinking induced exceeds the solubility threshold. The shape and size of the laser focus determine the geometry and size of individual volume elements (voxels). Voxels can have a transverse dimension as small as 100 nm when excitation is performed using an 800 nm, ultrafast laser (Lafratta et al., 2007; Sugioka and Cheng, 2014). MAP has fostered a revolution in the rapid prototyping and on-demand creation of parts with sub-micron resolution. For instance, MAP has been used for the fabrication of micromachines (Farrer et al., 2006), 3D photonic crystals (Rybin et al., 2015), microring resonators (Li et al., 2008), waveguides (Klein et al., 2005), microlasers (Yokoyama et al., 2003), and scaffolds for cell growth (Allen et al., 2005; Basu et al., 2005).

Typical photoinitiators in multiphoton photoresists exhibit positive contrast, meaning that the size of the fabricated features increases with decreasing fabrication velocity, or, equivalently, with increasing exposure. However, recently a number of photoinitiators have been shown to exhibit apparent "negative contrast" (Stocker et al., 2011). Photoresists formulated with such photoinitiators exhibit proportional velocity (PROVE) behavior (Stocker et al., 2011), i.e., the size of fabricated features increases with increasing fabrication velocity. PROVE materials open the door to new applications that demand higher precision in nanofabrication.

Here we present a study of MAP lithography in acrylic photoresists with the photoinitiator bis-[4-(diphenylamino) stryl]-1-(2-ethylhexyloxy), 4-(methoxy)benzene (KL68) (Devoe et al., 2011). We demonstrate that these photoresists exhibit PROVE behavior resulting from a novel mechanism, local heating. We show that the feature size in photoresists containing KL68 decreases substantially with an increase in temperature of less than 10°C. In contrast, in MAP photoresists based on conventional photoinitiators, the feature size decrease over this temperature range is minimal or non-existent, as observed previously by Kawata and co-workers (Takada et al., 2008). Our findings open the door to using thermal effects to achieve improved resolution in MAP.

Materials and methods

Sample preparation

The photoinitiators we examined included bis-[4-(diphenylamino) stryl]-1-(2-ethylhexyloxy), 4-(methoxy) benzene (KL68), Lucirin TPO-L, malachite green carbinol base (MGCB), and malachite green carbinol hydrochloride (MCB•HCl). KL68 (Figure 1A) was synthesized as reported previously (Leatherdale et al., 2007). Lucirin TPO-L, MGCB and MCB•HCl were purchased from Sigma Aldrich, and were used as received. Photoresist samples were prepared by mixing two monomers, which, unless otherwise noted, were tris (2-hydroxy ethyl) isocyanurate triacrylate (Sartomer 368) and ethoxylated trimethylolpropanetriacrylate (Sartomer 499), in a 1:1 weight ratio (SR368/499). This formulation was chosen for its low shrinkage and high adhesion (Baldacchini et al., 2004). Photoinitiators were dissolved in the monomer mix at the weight percentages discussed below. Because the 2-photon-absorption cross section of KL68 is substantially greater than that of the other photoinitiators used, the weight percent of KL68 used was considerably smaller so that the laser power used for exposure was similar for all photoresists. After preparation, each photoresist was placed in a sample vial and left on a rotator overnight. No attempt was made to remove oxygen or radical inhibitors from the photoresists, as our goal was to study the polymerization behavior under the conditions most often used in the laboratory.

#1 glass coverslips (Corning) were used as substrates for our experiments. The coverslips were first cleaned in an oxygen plasma for 4 min. The coverslips were then immersed in a solution of 93% ethanol, 5% distilled water, and 2% (3-acryloxypropyl) trimethoxysilane by volume for 14 h, following by rinsing in ethanol for 1 h and drying at 95°C for 1 h. This acrylation procedure promotes adhesion of polymerized structures.

A photoresist sample was mixed and filtered through a 0.2-μm-pore-diameter filter, after which one drop was placed on an acrylated cover slip. A coverslip was taped to a microscope slide, covered with another coverslip, and then mounted on a sample holder for MAP experiments. The piece of cellophane tape between the two coverslips set the thickness of the photoresist film at ~60 μm. After exposure, the unpolymerized resin was removed by rinsing twice in ethanol for 2 min each, and once in water for 2 min. After development, the samples were left to dry at room temperature. For examination with a scanning electron microscope (SEM), the coverslips were attached to a mount with carbon tape and covered with a ~20 nm platinum/palladium layer using a sputter coater.

Optical setup

MAP was performed with a tunable, mode-locked, Ti: sapphire oscillator (Coherent Mira 900-F) with a center wavelength of 800 nm, a pulse duration of ~150 fs, and a repetition rate of 76 MHz. For photodeactivation studies, a second, identical oscillator was used at 800 nm in continuous-

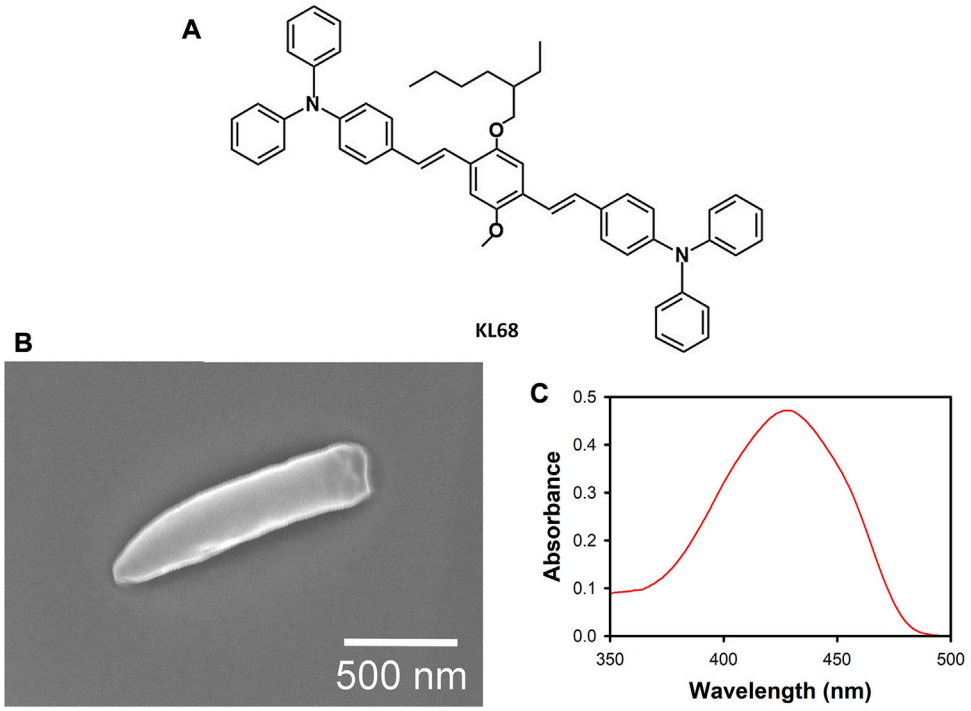

FIGURE 1
(A) The chemical structure of KL68. **(B)** A scanning electron micrograph of a representative fallen voxel from a KL68 photoresist at 24°C (see Figure 3A). **(C)** The UV/visible absorption spectrum of KL-68 in toluene (0.02 mM).

wave (CW) mode for inhibition of polymerization. The two beams were combined in a polarizing beam cube and directed to the sample through a 100 ×, 1.45 NA oil-immersion objective (Zeiss α Plan-FLUAR) mounted on an inverted microscope (Zeiss Axiovert 100). Cover slips with photoresist samples were mounted on a 3-axis piezoelectric stage (Physik Instrumente) for fine sample positioning in all dimensions. The piezo stage was attached to a motor-driven stage (Ludl Electronic Products, Ltd.) for coarse sample positioning. The movement of the piezo stage was controlled using a LabVIEW program, and fabrication was followed in real time using a CCD camera and a monitor. For reciprocity measurements, the minimum average power at which fabricated lines were observed was determined visually (Tomova et al., 2016) on the display screen. During all measurements, the axial position of the focal plane was kept fixed to ensure that a constant distance was maintained above the coverslip surface. For accurate measurement of the polymerization threshold powers, a reflected portion of the 800 nm beam (~5%) was chopped at a fixed frequency and was sent to a calibrated Si photodiode, the output of which was sent to a lock-in amplifier (Stanford Research Systems, SR810) referenced to the chopping frequency.

Temperature studies

The effect of temperature on polymerization efficiency was studied in photoresist samples containing KL68, MGCB, and Lucirin TPO-L. The temperature of each sample was controlled by an objective heater (Bioptechs Inc.). The sample was allowed to come to thermal equilibrium at each temperature before measurements were made.

For estimation of the voxel size through SEM analysis, we used the ascending scan method (Sun et al., 2002; Sun et al., 2003). Rows of voxels were fabricated for each photoresist and temperature. Every row contained 20 voxels, each of which was exposed for 0.5 s at a fixed laser power. This exposure time was chosen because in a typical radical photoresist the voxel dimensions (Sun et al., 2003) and the exposure threshold (Yang et al., 2019; Liaros and Fourkas, 2020) become relatively insensitive to small changes in exposure time, allowing for the creation of more reproducible voxels. The focal height above the substrate was increased by 100 nm for each consecutive voxel in the row. At some focal height, the voxel is attached only weakly to the surface, and so falls over upon development. An SEM of a representative fallen voxel that was used in the analysis below is shown in Figure 1B.

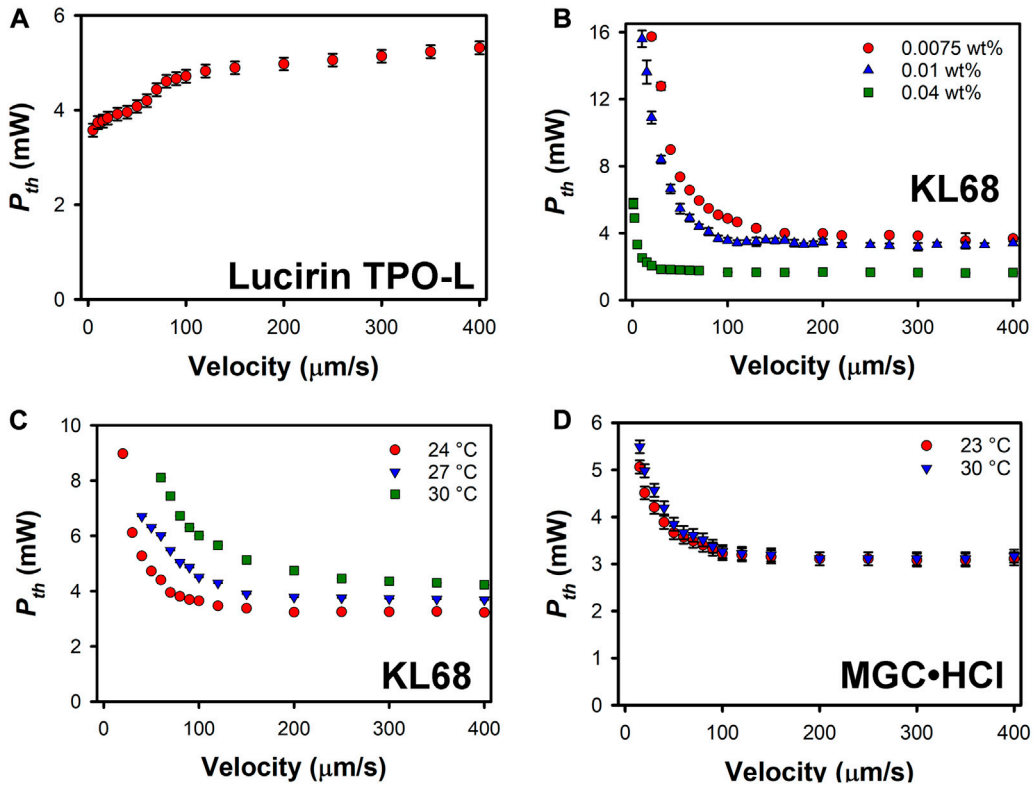

FIGURE 2
Threshold power as a function of velocity for **(A)** 1 wt% Lucirin TPO-L in 1:1 S368/499 at 24°C, **(B)** KL-68 at 0.0075 wt%, 0.01 wt%, and 0.04 wt% in 1:1 S368/499, **(C)** 0.01 wt% KL68 in 1:1 SR368/499 at 24°C, 27°C, and 30°C, and **(D)** 0.01 wt% MGC•HCl in 1:1 SR368/499 at 23°C and 30°C. In all experiments the excitation wavelength was 800 nm. The error bars represent the standard deviation in the exposure threshold based on multiple measurements. In some cases the error bars are smaller than the symbols.

Results

KL68 characterization

The UV/visible absorption spectrum of KL68 in toluene shows an absorption band centered at ~430 nm (Figure 1C). Based on this spectrum, we expect that 800 nm excitation should fall within the 2-photon absorption band for this material.

In the simplest model of exposure, the same exposure dose leads to the same degree of crosslinking, regardless of the exposure duration. Such behavior is known as reciprocity. In the case of 2-photon excitation, reciprocity implies that so long as the integral of the square of the irradiance over the exposure time is the same, then the degree of crosslinking should be the same. Reciprocity is only observed in radical photoresists in limited circumstances (Yang et al., 2019; Liaros and Fourkas, 2020). Nevertheless, the threshold power for polymerization in radical photoresists typically increases as the fabrication velocity increases (and thereby the exposure time decreases). Such behavior is observed, for instance, in a 1:1 SR368/499 photoresist containing the conventional, Norrish Type I radical photoinitiator, Lucirin TPO-L (Figure 2A). The threshold power depends strongly on fabrication velocity up to ~100 μm/s, after which the dependence becomes weaker. At even higher fabrication velocities the threshold power becomes nearly independent of velocity (Supplementary Figure S1A). The structure in the data at velocities below 100 μm/s hints at the existence of complex photopolymerization dynamics. Given our estimated beam diameter of 0.5 μm, the exposure time at a given point is approximately half of the inverse velocity in μm/s. A logarithmic plot of the threshold power as a function of the exposure time (Supplementary Figure S1B) is flat at exposure times between 0.1 and 1 ms. This behavior has been shown in similar systems to be due to oxygen diffusion occurring on a shorter time scale than exposure (Yang et al., 2019). At longer exposure times the power threshold decreases, which in similar systems has been attributed to diffusion of the initiator being faster than the exposure time (Yang et al., 2019). Interestingly, our data show two distinct periods of decreasing threshold within this time range; the source of this bimodal decrease is unclear. These results for Lucirin TPO-L can be viewed as baseline data for the typical polymerization dynamics of 1:1 SR368/499 photoresists.

Figure 2B shows the threshold power for polymerization as a function of fabrication velocity for three different concentrations of KL68 in a 1:1 SR368/499 photoresist. The polymerization threshold power decreases significantly as the fabrication velocity is increased, before levelling off at higher fabrication velocities. The higher the photoinitiator concentration, the lower the velocity at which the threshold power becomes insensitive to velocity. Corresponding logarithmic plots of the threshold power as a function of exposure time (Supplementary Figure S2) are flat at short times and grow linearly at longer times. The slopes in this latter region are similar for the two lower concentrations, and smaller for the highest concentration. The same behavior has been observed in photoresists with KL68 concentrations up to 0.1 wt%. Photoresists with even higher KL68 concentrations were not examined in detail due to their high photosensitivity, but the same PROVE behavior was still observed.

The data in Figure 2B; Supplementary Figure S2 indicate that in KL68 photoresists, longer exposure times result in less crosslinking than do shorter exposure times. In other words, KL68 endows PROVE behavior in these photoresists, implying that the light that drives the exposure also inhibits the exposure in some manner. As in other PROVE photoresists, the crosslinking must occur relatively slowly, such that at higher velocities the focal point moves away from an exposed region before crosslinking is complete, removing the source of inhibition and decreasing the exposure threshold (Stocker et al., 2011). In the PROVE materials explored previously, this behavior was attributed to the existence of a long-lived, photodeactivatable state in the photoinitiation pathway. In such a case, deactivation is driven by linear absorption of the same laser that drives multiphoton excitation in the photoinitiator (Stocker et al., 2011).

To check for the presence of this phenomenon, a CW beam of the same wavelength as the mode-locked excitation beam can be employed simultaneously (Li et al., 2009). In the case of KL68 photoresists, addition of a CW, 800 nm beam with a power of up to 120 mW during the 800 nm, 2-photon excitation of the KL68 photoresists at an average laser power of 12 mW did not have any impact on the exposure threshold. This finding indicates that photodeactivation of electronic states is not the mechanism underlying the PROVE behavior in this system, and that ultrafast pulses are essential to deactivation.

Temperature studies

As an alternative hypothesis, we explored whether local heating by the excitation beam is responsible for the observed PROVE behavior. Such heating arises primarily from effects precipitated by absorption to an excited electronic state, such as intramolecular vibrational relaxation and solvation. Therefore, when there is no linear absorption at the excitation wavelength, heating is only significant upon ultrafast pulsed excitation, which can drive multiphoton absorption. Heating during exposure has been demonstrated to be modest in a representative multiphoton photoresist, on the order of a few °C (Mueller et al., 2013). Such a small temperature increase would not typically be expected to have a significant effect on the polymerization threshold or the feature size (Takada et al., 2008). To determine whether thermal effects play a role in the KL-68 photoresists studied here, an objective heater was used to control the sample temperature. The threshold power for polymerization was measured as a function of fabrication velocity in a sample containing 0.01 wt% KL 68 in 1:1 SR368/499 at 24°C, 27°C, and 30°C. The data in Figure 2C demonstrate that the polymerization threshold increases significantly between 24°C and 30°C at all velocities examined. At all temperatures, the polymerization threshold decreases as the fabrication velocity increases from 20 μm/s to 300 μm/s, and then remains independent of velocity for fabrication velocities up to the highest measured here, 1 cm/s (see also Supplementary Figure S3A). Corresponding logarithmic plots of the threshold power as a function of exposure time are shown in Supplementary Figure S3B.

As a control, we performed temperature-dependent experiments in photoresists containing either Lucirin TPO-L or MGC•HCl as the photoinitiator in 1:1 SR368/499. Lucirin TPO-L is a conventional radical photoinitiator, and at 1 wt% in the photoresist we observed no statistically significant difference in the polymerization threshold between 23°C and 30°C. As shown in Figures 2A,D, a photoresist containing 0.25 wt% MGC•HCl exhibits PROVE behavior at both 23°C and 30°C, and there is no statistically significant difference between the data at the two temperatures. The corresponding logarithmic plots of the threshold power as a function of exposure time are shown in Supplementary Figure S4.

The above results indicate that thermal effects have a strong impact on the photopolymerization dynamics of KL68 photoresists as compared to conventional photoinitiators, and even to PROVE photoinitiators studied previously. To investigate whether temperature influences the feature size, we studied the voxel dimensions as a function of temperature in a 0.01 wt% KL68 photoresist. To create the voxels, we chose a laser power that was above the polymerization threshold at 24°C, and that did not cause any sample damage for an exposure time of 0.5 s, which is comparable to the longest exposure times used in Figure 3. With increasing temperature, reference lines and voxels became less visible, indicating a lower polymerization rate.

Figure 3A shows the voxel height and width as a function of temperature for this photoresist. Both the average voxel height and width decrease with increasing temperature. A temperature increase of 3 °C causes the average voxel height to go from ~1,150 nm to ~980 nm, a decrease of ~17%. The average voxel width goes from ~310 to ~270 nm, a decrease of ~15%. Above 27°C, no polymerization was observed at the laser power used.

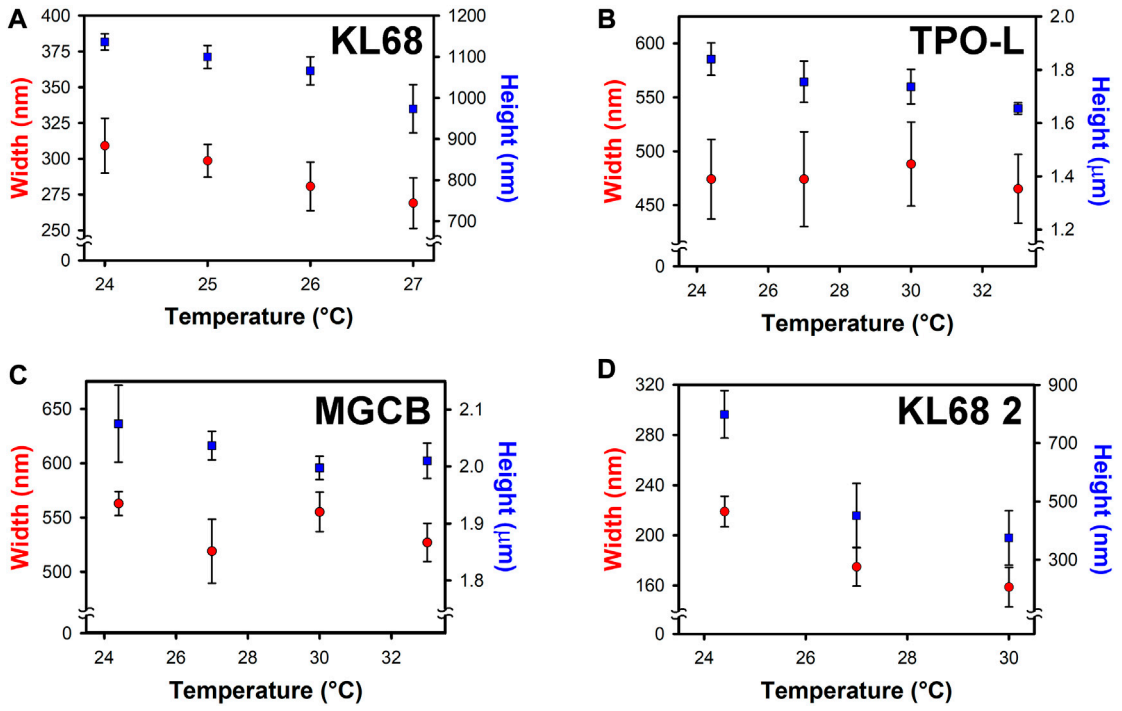

FIGURE 3
Temperature dependence of the voxel height (squares) and width (circles) in a photoresist composed of **(A)** 0.05 wt% KL68 in 1:1 SR368/499 at a fixed irradiance and exposure time. **(B)** Voxel size temperature dependence for 3 wt% Lucirin TPO-L in 1:1 SR368/499. **(C)** Voxel size temperature dependence for 1.5 wt% MGCB in 1:1 SR368/499. **(D)** Voxel size temperature dependence for 0.05 wt% KL68 in a 3:1 mixture of SR351/285. The error bars represent ±1 standard deviation as determined by measuring at least 10 voxels in each case.

To determine whether the observed temperature dependence arises from the photoresist or from the photoinitiator, we performed control experiments with the same monomer mixture using either Lucirin TPO-L or MGCB as the photoinitiator. As shown in Figure 3B, for a 3 wt% Lucirin TPO-L photoresist the average voxel width was nearly constant throughout this temperature range. Some of the voxels were deformed, resulting in a larger deviation in the mean voxel dimensions than in the case of the KL68 photoresist. The results for a 1.5 wt% MGCB photoresist are shown in Figure 3C. The average widths of the voxels ranged between ~560 nm at the lowest temperature to ~520 nm at the highest temperature, a decrease of ~8%. The average voxel height ranged from 2.08 μm at the lowest temperature to 2.00 μm at the highest temperature, a decrease of ~4%. The fact that the two control photoresists exhibit considerably smaller, and likely statistically insignificant, changes in voxel dimensions over a temperature range that is twice as large as the one accessible for the KL68 photoresist indicates that although the photoresist composition might play a minor role in the temperature-dependent behavior of the KL68 photoresists, the photoinitiator itself is the most important contributor. To explore this effect further, we studied KL68 photoresists formulated with different monomers. In Figure 3D we present the voxel dimensions from photoresists that contained 0.05 wt% KL68 in a 3:1 by weight mixture of trimethylolpropane triacrylate (SR351) and tetrahydrofurfuryl acrylate (SR285). Increasing the temperature from 24°C to 30°C causes the average voxel height to decrease by approximately 50%, from ~800 to ~400 nm, and the average width to decrease by ~38%, from ~220 to ~160 nm.

Discussion

The data presented here indicate that the PROVE behavior observed in radical photoresists that incorporate KL68 as the photoinitiator is thermal in origin, in contrast to previously reported photoinitiators in which PROVE behavior arises from photodeactivation of a long-lived intermediate. Furthermore, our experiments demonstrate that this thermal effect can be harnessed to enhance resolution in MAP.

For the same monomer mixture, the results of temperature-dependent exposure-threshold and voxel-size experiments with KL68 as the photoinitiator differ substantially from those for the control photoinitiators, Lucirin TPO-L, MGCB, and MGC•HCl. The magnitude of the thermal effect with KL68 is also dependent

on the monomer mixture. These results all support the conclusion that the initiation mechanism for KL68 differs from that of the other photoinitiators studied here. Lucirin TPO-L is a classic, Norrish Type I photoinitiator that undergoes photolysis to create reactive radicals upon electronic excitation (Roffey, 1982). MGCB and MGC•HCl are both believed to eject electrons upon photoexcitation (Stocker et al., 2011). These electrons are solvated in the photoresist, eventually leading to the initiation of radical photopolymerization. Deactivation for these photoinitiators is photoinduced, and is believed to result from back transfer of the solvated electrons (Li et al., 2009).

Photoinitiators such as KL68 are believed to induce radical polymerization *via* the transfer of an electron to a monomer (Cumpston et al., 1999). When an electron is transferred to another molecule, as opposed to being solvated within the photoresist, photoinduced back transfer with near-infrared light may not be able to occur. Furthermore, if polymerization were initiated immediately upon electron transfer, then a reduced rate of polymerization at an increased temperature would be indicative of a decreased electron-transfer rate. Although such a scenario is not impossible, the magnitude of the decrease in polymerization rate in the second photoresist studied here renders this possibility unlikely given that the electron transfer is photoinduced, and therefore would not be expected to have a high barrier (Marcus, 1993).

The most likely explanation for our results is that photoinduced electron transfer from the photoinitiator to a monomer creates a weakly reactive species that can eventually lead to a crosslinking reaction. In this scheme, the mechanism of deactivation would be thermally-induced electron back transfer. Regenerating the neutral photoinitiator in its ground state is an exergonic process, but a barrier must be overcome for this back transfer to occur. The strong temperature dependence of the thermal deactivation rate further suggests that the Gibbs free energy of activation for the back-transfer process is high, a situation that is not uncommon (Marcus, 1993).

The two KL68 photoresist compositions investigated here exhibit substantially different temperature sensitivities. The viscosity of the SR499/SR368 photoresist is orders of magnitude greater than that of the SR351/SR285 photoresist, although both photoresists are more viscous than typical solvents. It is therefore somewhat surprising that the SR351/SR285 photoresist exhibits the stronger temperature dependence in the polymerization rate. A lower viscosity should lead to a greater rate of cage escape for the geminate ion pair created by photoinduced electron transfer (Olmsted and Meyer, 1987). If anything, this rate should increase modestly at higher temperature. Because cage escape prevents back transfer, a higher temperature should increase the efficiency of photoinitiation. We estimate the viscosity of the SR351/SR285 photoresist to be 80 cP, which may be high enough to minimize the importance of cage escape.

The energetics of the electron-transfer process depends upon the species involved. Because the electron must be transferred from an excited KL68 molecule to a monomer, changing the monomers will change the energetics. The SR351/SR285 photoresist may therefore have a higher Gibbs free energy of activation for back transfer, which would lead to a stronger temperature dependence for the voxel size.

We should also consider the fact that the SR351/SR285 photoresist forms a polymer with a considerably lower degree of crosslinking than that created by the SR499/SR368 photoresist, given that the SR285 monomer contains only a single acrylate group. Thus, the gelation point of the SR351/SR285 photoresist occurs at a higher degree of conversion than is the case for the SR499/SR368 photoresist. This difference may also lead to a higher degree of sensitivity to the kinetics of the photoinitiation process in the SR351/SR285 photoresist.

Conclusion

We have studied MAP in acrylic photoresists incorporating the photoinitiator KL68. We find that photoresists containing KL68 exhibit PROVE behavior, which means that the size of fabricated features increases with increasing fabrication velocity. The mechanism for PROVE behavior with KL68 is different from that of previously studied PROVE photoinitiators. In particular, the polymerization efficiency in KL68-based photoresists exhibits a strong temperature dependence.

KL68 is one of many push-pull molecules with high 2-photon absorption cross sections that have been developed as photoinitiators for MAP (Cumpston et al., 1999; Malval et al., 2009; Nazir et al., 2013). Such molecules typically initiate polymerization *via* photoinduced electron transfer, and so may also exhibit the type of temperature-dependent behavior observed here. It would be interesting to explore thermal PROVE behavior in other such systems. The energetics of back transfer, and therefore the temperature dependence of the process, can be tuned by varying both the photoinitiator and the monomers. Still, further work is required to ascertain the exact mechanism of resolution enhancement so that the potential of this phenomenon can be harnessed to full advantage. It will also be of interest to explore whether species such as oxygen and radical inhibitors influence the thermal effects described here. This new mechanism for PROVE behavior presents an intriguing new path towards controlling and improving resolution in MAP.

Data availability statement

The raw data supporting the conclusion of this article will be made available by the authors, without undue reservation.

Author contributions

NL, ZT, SG, RD, BG, DE, and JF contributed to conception and design of the study. NL, ZT, SG, JB, and AS performed the investigation and analyzed the data. NL, ZT, and JF wrote the original draft, and NL, ZT, SG, RD, BG, DE, and JF reviewed and edited the manuscript. JF supervised the project.

Funding

NL acknowledges support by the Research Corporation for Science Advancement (RCSA) and the National Science Foundation (NSF) through a Cottrell Fellowship. The Cottrell Fellowship Initiative is partially funded by a National Science Foundation award to RCSA (CHE-2039044).

Conflict of interest

RD, BG, and DE were employed by 3M Co.

The remaining authors declare that the research was conducted in the absence of any commercial or financial relationships that could be construed as a potential conflict of interest.

Publisher's note

Supplementary material

The Supplementary Material for this article can be found online at: https://www.frontiersin.org/articles/10.3389/fnano.2022.988997/full#supplementary-material

References

Allen, R., Nielson, R., Wise, D. D., and Shear, J. B. (2005). Catalytic three-dimensional protein architectures. *Anal. Chem.* 77, 5089–5095. doi:10.1021/ac0507892

Baldacchini, T., Lafratta, C. N., Farrer, R. A., Teich, M. C., Saleh, B. E. A., Naughton, M. J., et al. (2004). Acrylic-based resin with favorable properties for three-dimensional two-photon polymerization. *J. Appl. Phys.* 95, 6072–6076. doi:10.1063/1.1728296

Basu, S., Cunningham, L. P., Pins, G. D., Bush, K. A., Taboada, R., Howell, A. R., et al. (2005). Multiphoton excited fabrication of collagen matrixes cross-linked by a modified benzophenone dimer: Bioactivity and enzymatic degradation. *Biomacromolecules* 6, 1465–1474. doi:10.1021/bm049258y

Campbell, M., Sharp, D. N., Harrison, M. T., Denning, R. G., and Turberfield, A. J. (2000). Fabrication of photonic crystals for the visible spectrum by holographic lithography. *Nature* 404, 53–56. doi:10.1038/35003523

Camposeo, A., Persano, L., Farsari, M., and Pisignano, D. (2019). Additive manufacturing: Applications and directions in photonics and optoelectronics. *Adv. Opt. Mat.* 7, 1800419. doi:10.1002/adom.201800419

Cumpston, B. H., Ananthavel, S. P., Barlow, S., Dyer, D. L., Ehrlich, J. E., Erskine, L. L., et al. (1999). Two-photon polymerization initiators for three-dimensional optical data storage and microfabrication. *Nature* 398, 51–54. doi:10.1038/17989

Devoe, R. J., Lee, T.-C., Larsen, J. K., Ender, D. A., Sahlin, J. J., Sykora, C. R., et al. (2011). "High photosensitivity two-photon photoresists for large area surface microstructuring," in *MRS Proceedings*. Cambridge, UK: Cambridge University Press, 1365, pp. mrss11–1365-tt09–14

Farrer, R. A., Lafratta, C. N., Li, L., Praino, J., Naughton, M. J., Saleh, B. E., et al. (2006). Selective functionalization of 3-D polymer microstructures. *J. Am. Chem. Soc.* 128, 1796–1797. doi:10.1021/ja0583620

Finkbeiner, S. (2013). "Mems for automotive and consumer electronics," *MRS Proceedings*. Cambridge, UK: Cambridge University Press, 1365, pp. mrss11–1365-tt09–14

Fourkas, J. T., Gao, J., Han, Z., Liu, H., Marmiroli, B., Naughton, M. J., et al. (2021). Grand challenges in nanofabrication: There remains plenty of room at the bottom. *Front. Nanotechnol.* 3, 700849. doi:10.3389/fnano.2021.700849

Klein, S., Barsella, A., Leblond, H., Bulou, H., Fort, A., Andraud, C., et al. (2005). One-step waveguide and optical circuit writing in photopolymerizable materials processed by two-photon absorption. *Appl. Phys. Lett.* 86, 211118. doi:10.1063/1.1915525

Lafratta, C. N., Fourkas, J. T., Baldacchini, T., and Farrer, R. A. (2007). Multiphoton fabrication. *Angew. Chem. Int. Ed.* 46, 6238–6258. doi:10.1002/anie.200603995

Leatherdale, C. A., Schardt, C. R., Thompson, D. S., and Thompson, W. L. (2007). *Multi-photon reactive Compositions with inorganic Particles and Method for fabricating structures*. US 2007/0264501 A1. United States patent application.

Li, L., Gattass, R. R., Gershgoren, E., Hwang, H., and Fourkas, J. T. (2009). Achieving Λ/20 resolution by one-color initiation and deactivation of polymerization. *Science* 324, 910–913. doi:10.1126/science.1168996

Li, L., Gershgoren, E., Kumi, G., Chen, W.-Y., Ho, P. T., Herman, W. N., et al. (2008). High-performance microring resonators fabricated with multiphoton absorption polymerization. *Adv. Mat.* 20, 3668–3671. doi:10.1002/adma.200800032

Liaros, N., and Fourkas, J. T. (2020). Methods for determining the effective order of absorption in radical multiphoton photoresists: A critical analysis. *Laser Phot. Rev.* 15, 2000203. doi:10.1002/lpor.202000203

Malval, J.-P., Morlet-Savary, F., Chaumeil, H., Balan, L., Versace, D.-L., Jin, M., et al. (2009). Photophysical properties and two-photon polymerization ability of a nitroalkoxystilbene derivative. *J. Phys. Chem. C* 113, 20812–20821. doi:10.1021/jp9075977

Marcus, R. A. (1993). Electron transfer reactions in chemistry: Theory and experiment (nobel lecture). *Angew. Chem. Int. Ed. Engl.* 32, 1111–1121. doi:10.1002/anie.199311113

Mueller, J. B., Fischer, J., Mange, Y. J., Nann, T., and Wegener, M. (2013). *In-situ* local temperature measurement during three-dimensional direct laser writing. *Appl. Phys. Lett.* 103, 123107. doi:10.1063/1.4821556

Nazir, R., Danilevicius, P., Gray, D., Farsari, M., and Gryko, D. T. (2013). Push–pull acylo-phosphine oxides for two-photon-induced polymerization. *Macromolecules* 46, 7239–7244. doi:10.1021/ma4010988

Ngo, T. D., Kashani, A., Imbalzano, G., Nguyen, K. T. Q., and Hui, D. (2018). Additive manufacturing (3d printing): A review of materials, methods, applications and challenges. *Compos. Part B Eng.* 143, 172–196. doi:10.1016/j.compositesb.2018.02.012

Olmsted, J., and Meyer, T. J. (1987). Factors affecting cage escape yields following electron-transfer quenching. *J. Phys. Chem.* 91, 1649–1655. doi:10.1021/j100290a071

Pan, T., and Wang, W. (2011). From cleanroom to desktop: Emerging micro-nanofabrication technology for biomedical applications. *Ann. Biomed. Eng.* 39, 600–620. doi:10.1007/s10439-010-0218-9

Roffey, C. G. (1982). *Photopolymerization of surface coatings*. New York: Wiley-Interscience.

Rybin, M., Shishkin, I., Samusev, K., Belov, P., Kivshar, Y., Kiyan, R., et al. (2015). Band structure of photonic crystals fabricated by two-photon polymerization. *Crystals* 5, 61–73. doi:10.3390/cryst5010061

Stocker, M. P., Li, L., Gattass, R. R., and Fourkas, J. T. (2011). Multiphoton photoresists giving nanoscale resolution that is inversely dependent on exposure time. *Nat. Chem.* 3, 223–227. doi:10.1038/nchem.965

Sugioka, K., and Cheng, Y. (2014). Femtosecond laser three-dimensional micro- and nanofabrication. *Appl. Phys. Rev.* 1, 041303. doi:10.1063/1.4904320

Sun, H.-B., Takada, K., Kim, M.-S., Lee, K.-S., and Kawata, S. (2003). Scaling laws of voxels in two-photon photopolymerization nanofabrication. *Appl. Phys. Lett.* 83, 1104–1106. doi:10.1063/1.1599968

Sun, H.-B., Tanaka, T., and Kawata, S. (2002). Three-dimensional focal spots related to two-photon excitation. *Appl. Phys. Lett.* 80, 3673–3675. doi:10.1063/1.1478128

Takada, K., Kaneko, K., Li, Y.-D., Kawata, S., Chen, Q.-D., and Sun, H.-B. (2008). Temperature effects on pinpoint photopolymerization and polymerized micronanostructures. *Appl. Phys. Lett.* 92, 041902. doi:10.1063/1.2834365

Tomova, Z., Liaros, N., Gutierrez Razo, S. A., Wolf, S. M., and Fourkas, J. T. (2016). *In situ* measurement of the effective nonlinear absorption order in multiphoton photoresists. *Laser Phot. Rev.* 10, 849–854. doi:10.1002/lpor.201600079

Wu, S.-Y., Yang, C., Hsu, W., and Lin, L. (2015). 3d-Printed microelectronics for integrated circuitry and passive wireless sensors. *Microsyst. Nanoeng.* 1, 15013. doi:10.1038/micronano.2015.13

Yang, L., Münchinger, A., Kadic, M., Hahn, V., Mayer, F., Blasco, E., et al. (2019). On the schwarzschild effect in 3d two-photon laser lithography. *Adv. Opt. Mat.* 7, 1901040. doi:10.1002/adom.201901040

Yokoyama, S., Nakahama, T., Miki, H., and Mashiko, S. (2003). Two-photon-induced polymerization in a laser gain medium for optical microstructure. *Appl. Phys. Lett.* 82, 3221–3223. doi:10.1063/1.1573350